Thin Solid Films 550 (2014) 36–39

Contents lists available at ScienceDirect

Thin Solid Films

journal homepage: www.elsevier.com/locate/tsf

A comparative study of Cu_2ZnSnS_4 thin films growth by successive ionic layer adsorption–reaction and sol-gel methods

S. Kahraman *, S. Çetinkaya, H.A. Çetinkara, H.S. Güder

Semiconductor Research Laboratory, Physics Department, Faculty of Art and Science, Mustafa Kemal University, 31034 Hatay, Turkey

ARTICLE INFO

Article history:
Received 14 April 2013
Received in revised form 8 October 2013
Accepted 8 October 2013
Available online 16 October 2013

Keywords:
Thin films
Copper zinc tin sulfide
Sol-gel
Successive ionic layer adsoprtion-reaction
Sulfurization

ABSTRACT

Owing to the high natural abundance and non-toxicity of all the constituents, the copper–zinc–tin–sulfide compound has been attracting attention in recent years for the production of cheap solar absorber materials. Solution-based low-cost approaches are being developed for the deposition of this compound. In this comparative study, we have investigated Cu_2ZnSnS_4 thin films prepared by using successive ionic layer adsorption–reaction and sol-gel methods. X-ray diffraction studies indicated the polycrystalline nature of the films. No secondary phases were observed. The sol-gel grown Cu_2ZnSnS_4 film was found to have smaller crystallite size and higher micro-strain and dislocation density values. Phase purity and good crystalline quality of the studied films were proved through the Raman studies. From the scanning electron microscopy images, sol-gel grown Cu_2ZnSnS_4 film was found to have more homogenous and smooth morphology. Possible chemical formula of the films was determined. The optical absorption of the sol-gel grown film covered a wider wavelength range by means of absorbing more visible photons. The optical band gap values were estimated to be 1.45 and 1.40 eV for the successive ionic layer adsorption–reaction and sol-gel grown samples, respectively. It was concluded that both methods are effective and can be used to produce high-quality Cu_2ZnSnS_4 thin films for cheap and green solar cell applications.

1. Introduction

Thin-film chalcogen materials, especially $CuInSe_2$, $Cu(In,Ga)(S,Se)_2$ (CIGS) and CdTe, are currently used in the production of large-scale, commercial, photovoltaic devices. However, the scarcity of indium and tellurium in the earth's crust limits the future of CIGS- and CdTe-based solar cells. In addition, the price of In and relatedly solar-cell production costs will increase in the near future due to the extensive use of indium in display technologies and opto-electronic devices. Another problem with CdTe-based solar cells is that the cadmium (Cd) is very toxic to health and the environment. This problem has led researchers to search for more abundant and greener materials. Because of its similar properties to the CIGS compound, the I_2–II–IV–VI_4 group as the basis for absorber materials has been attracting attention. The Cu_2ZnSnS_4 (CZTS) compound is a good candidate for photovoltaic applications as an absorber layer [1–4]. CZTS has a direct band gap ranging from 1.4 to 1.6 eV which is close to the optimum value required for a solar cell's absorber layer, a high absorption coefficient in the visible solar spectrum wavelengths and a p-type conductivity [5]. However, even though it is a promising absorber material, the studies on CZTS-based solar cells are at an early stage [6]. Aqueous solution deposition methods have several advantages, very important one being that a variety of thin films can be grown at low temperatures using cheap manufacturing equipment. Among others, successive ionic layer adsorption–reaction (SILAR) and sol-gel spin-coating methods are very simple, effective and low-cost processes. In a SILAR deposition process, the substrate is immersed successively into separated cationic and anionic precursor solutions. This allows the conformal deposition of extremely thin sulfide layers with a control of the thickness even down to about 1 nm [7]. A sol-gel process is based on hydrolysis and poly-condensation reactions. Sulfide films can be directly obtained by sulfurizing oxyhydrate precursors. To date, several groups have reported CZTS thin films produced via the SILAR and sol-gel methods [8–15]. In this comparative study, we prepared CZTS thin films on soda lime glass substrates by using SILAR and sol-gel spin-coating methods and investigated structural, morphological, compositional and optical characteristics of the films.

2. Experimental details

Soda lime glass substrates were used as substrates which were ultrasonically cleaned in turn with detergent, nitric acid (1:4), acetone, ethanol for 10 min and drying at 100 °C for 1 h. It is well known that copper tends to make secondary phases [16,17]. Cu–Zn–Sn–S compounds should be grown under Cu-poor conditions to prevent $Cu_{2-x}S$ or other binary/ternary phases and to improve the performance of the film because Cu-poor conditions enhance the formation of Cu vacancies, which give rise to shallow acceptors. Another reason to use copper poor composition is some Sn loss which occurs during the sulfurization process, mainly in the form of SnS [18]. In this study, therefore, we prepared Cu-poor solutions in both methods. The SILAR grown CZTS

* Corresponding author. Tel.: +90 3262455845x1637; fax: +90 3262455867.
E-mail address: suleymanmku@gmail.com (S. Kahraman).

0040-6090/$ – see front matter © 2013 Elsevier B.V. All rights reserved.
http://dx.doi.org/10.1016/j.tsf.2013.10.035

thin films were obtained by sulfurizing Cu_2SnS_3/ZnS stacked sulfide layers deposited at room temperature. For the deposition of the Cu_2SnS_3 layer the cation solution was composed of 0.005 M $CuCl_2$ (Aldrich 97%) and 0.01 M $SnCl_2$ (Merck 98%). To adjust the pH value of the solution, triethanolamin (Alfa Aesar, 98 +%) was used. For the deposition of the ZnS layer on the Cu_2SnS_3 layer, the cation solution contained 0.1 M $ZnCl_2$ (Alfa Aesar 98 +%). To adjust pH value of the $ZnCl_2$ solution, diluted sulfuric acid (Sigma-Aldrich 95–97%) was used. Both anion solutions were prepared with 0.05 M $Na_2S{\cdot}9H_2O$ (Alfa Aesar 98.0%) serving as a source of sulfur. The number of immersion cycles for the Cu_2SnS_3 and ZnS layers was 30 and 40, respectively.

To produce CZTS thin films by using sol-gel spin-coating method, sol solutions were prepared by dissolving copper (II) acetate monohydrate (0.3 M, 98 +%), zinc (II) acetate dihydrate (0.3 M, 99.99%), tin (II) chloride (0.3 M, 98%) from Sigma-Aldrich and thiourea (1.2 M, 99.0 +% from Sigma-Aldrich) into 2-methoxyethanol (20 ml, 99.8% from Sigma-Aldrich). The final solution was stirred at 45 °C, 850 rpm for 1 h to dissolve the metal compounds completely. During stirring, 2 ml of diethanolamine (DEA) was dropped slowly into the solution as a stabilizer. The prepared solution was spin-coated onto the substrate at 3000 rpm for 30 s followed by solvent-drying at 175 °C for 10 min on a hot plate. The spin-coating and solvent-drying processes were repeated 10 times to obtain the desired thickness of the film.

After the deposition processes, the samples were subjected to an annealing procedure at 500 °C for 2 h. Before the annealing, the tube furnace was evacuated to 5×10^{-2} Pa. Due to the high vapor pressure of sulfur at the annealing temperature, 30 g of elemental sulfur in an alumina crucible was put into the tube underneath the samples to compensate for any possible sulfur loss during the annealing. The heating rate was 5 °C/min. After the annealing process, the samples were allowed to cool naturally to room temperature. Through the cross-sectional electron microscopy imaging, thicknesses of the films were measured as 1.3 and 1.7 μm for the SILAR and sol-gel grown films, respectively. The crystal structure surface morphology, chemical composition and optical properties of the samples were examined by X-ray diffraction (XRD, PANalytical X'Pert PRO MPD with a wavelength of 1.5418 Å Cu Kα radiation), Raman spectroscopy (Confocal raman spectrometer, Witec alpha 300 with 532 nm light source), field-emission-scanning electron microscopy (FEG-SEM, Jeol JSM-7600F), energy dispersive x-ray spectroscopy (EDS, Oxford Instruments ISIS 300) and absorbance spectroscopy (UV/Vis/NIR spectroscopy, Lambda 950 with 150 mm integrating sphere) methods.

3. Results and discussions

3.1. Structural properties

The structural characterization was performed using X-ray diffraction (XRD) and Raman techniques. The diffraction patterns were obtained at a 40-keV of operating voltage and a 35-mA current. The step size and the scan step time were 0.0330° and 1 s, respectively. Fig. 1 shows the obtained XRD patterns of the CZTS samples. In the patterns of the samples, five peaks were observed at $2\theta = 18.25°$, 28.53°, 32.99°, 47.40° and 56.21°. The patterns of the samples match very well with Cu_2ZnSnS_4 (JCPDS 00-026-0575: tetragonal, $a = b = 5.427$ nm, $c = 10.848$ nm, I-42 m). The patterns prove that the crystallization process of the films is carried out after vacuum-sulfurization step. The reference patterns of the common possible secondary phases were also given for comparison in Fig. 1. No other prominent peaks were observed, which suggests that no secondary phases were present. The mean crystallite sizes (D) of the films were calculated from the peak width at the half maximum of a peak (β) using the Debye–Scherrer's equation [19]:

$$D = \frac{0.94\,\lambda}{\beta \cos\theta} \tag{1}$$

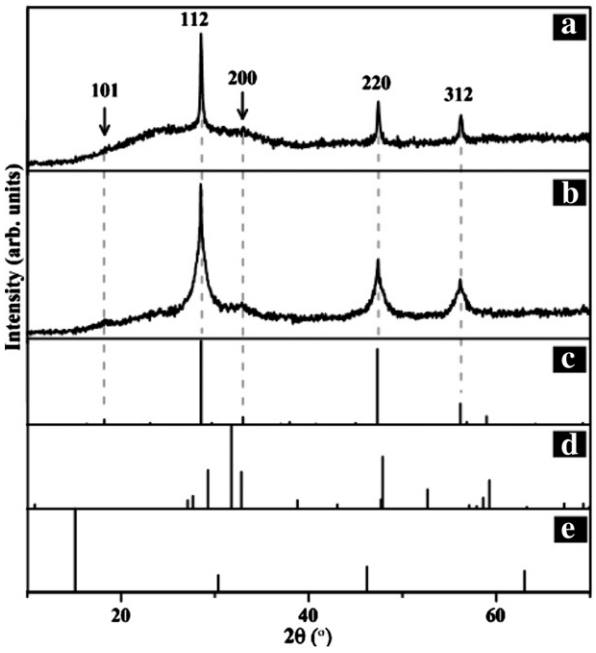

Fig. 1. The obtained XRD patterns of (a) SILAR grown and (b) sol-gel grown CZTS films and reference XRD patterns of possible secondary phases (c) Cu2ZnSnS4, 00-026-0575 (tetragonal, I-42 m) and (d) Cu2-xS, 00-024-0060 (covellite, P63/mmc) (e) SnS, 00-022-0950.

where λ is the wavelength of X-ray radiation, θ is the Bragg's angle of the 002 peak, and β is the angular width of the peak at full width at half maximum (FWHM) which can be obtained through a diffractometer. Mean crystallite size of the SILAR and sol-gel grown films (D) were calculated to be 20 ± 1 and 9 ± 1 nm, respectively. It is a well known information that each peak obtained in a diffractometer is broadened due to instrumental and physical factors (crystallite size and lattice strains) [20]. Therefore, the micro-strain (ε) and dislocation density (ρ) for an orientation can be estimated using 2θ and FWHM value (β) of the related peak. The corresponding formulas are given below [21,22]:

$$\varepsilon = \beta \cos\theta/4 \tag{2}$$

and

$$\rho = 1/D^2 \tag{3}$$

The estimations were done by taking into account each diffraction peak and the obtained average values are given in Table 1. It was found that the sol-gel grown CZTS film has smaller crystallite size and relatedly higher micro-strain and dislocation density values than those of SILAR grown CZTS film.

Binary or ternary sulfides such as ZnS and $Cu_{2-x}S$ have similar diffraction patterns to CZTS owing to their similar zinc blend-type structures. To prove the phase purity or to detect the presence of other possible secondary phases, Raman spectroscopy analyses of the samples over the range 200 to 500 cm^{-1} were also made and the results

Table 1
Estimated structural parameters and optical band gap values of the CZTS films.

Sample	Mean crystallite size (D) (nm)	Microstrain (ε) $\times 10^{-4}$	Dislocation density (ρ) $\times 10^{15}$ (m^{-2})	Estimated optical band gap value (eV)
SILAR grown CZTS	20 ± 1	18	2.5 ± 0.1	1.45
Sol-gel grown CZTS	9 ± 1	39	12.3 ± 0.1	1.40

are given in Fig. 2. In the Raman spectrum, an obvious major peak at 331 cm^{-1} and a minor peak at 368 cm^{-1} can be clearly seen. These spectral data are in good agreement with the reported Raman spectra of CZTS [23–25] and confirm the formation of the CZTS phase. Moreover, the strong major peak is an indication of the good crystalline quality of the compound. It is noticeable that the peaks at 351 and 274 cm^{-1} corresponding to ZnS, the peak at 475 cm^{-1} corresponding to $Cu_{2-x}S$ and the peak at 345 cm^{-1} corresponding to ZnS:Cu [26–28] do not appear, suggesting the absence of these compounds.

3.2. Morphological and compositional analysis

Top-view FEG-SEM images of the CZTS films are given in Fig. 3. From Fig. 3, it is clear that the sol-gel grown film (Fig. 3b) has more homogenous and smooth morphology than the SILAR grown film.

The results of the semi-quantitative, energy-dispersive X-ray spectroscopy (EDXS) analysis, which just illustrate the atomic fraction (a.f.) of each constituent elements of the CZTS films, are presented in Table 2. It is estimated from the elemental composition results normalized on eight atoms per formula unit of CZTS that the studied SILAR and sol-gel grown CZTS films can be formulated to be $Cu_{1.99}Zn_{1.25}Sn_{1.00}S_{3.76}$ and $Cu_{1.61}Zn_{1.30}Sn_{1.17}S_{3.94}$, respectively.

3.3. Optical properties

The absorption coefficient (α) of the films was calculated from the measured values of the reflectance (R) and transmittance (T) data using the relation [29]:

$$\alpha(\lambda) = \frac{1}{t}\ln\left[\frac{1-R(\lambda)}{T(\lambda)}\right] \quad (4)$$

where α is the absorption coefficient, t is the thickness of the sample and λ is the photon wave length. The calculated absorption coefficient values are of the order of 10^4 cm^{-1}. Near the absorption edge or in the strong absorption zone of the transmittance spectra, the absorption coefficient is related to the optical energy gap, E_g following the power-law behavior of Tauc's relation [30]

$$(\alpha h\nu) = B\left(h\nu - E_g\right)^m \quad (5)$$

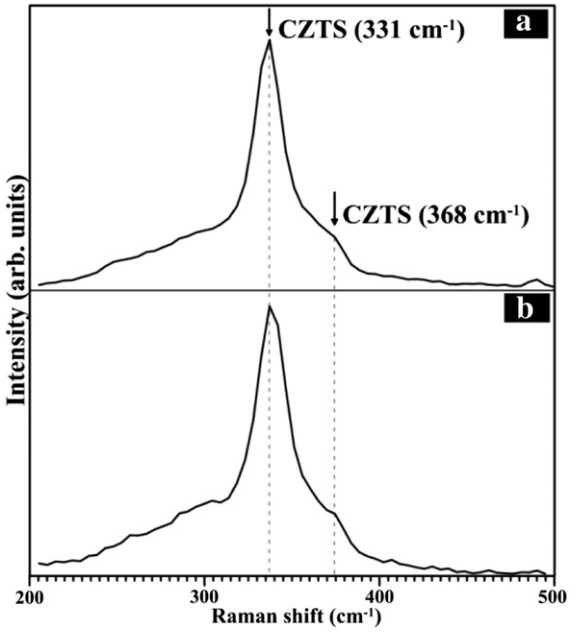

Fig. 2. Raman spectroscopy analyses of the (a) SILAR grown and (b) sol-gel grown CZTS films.

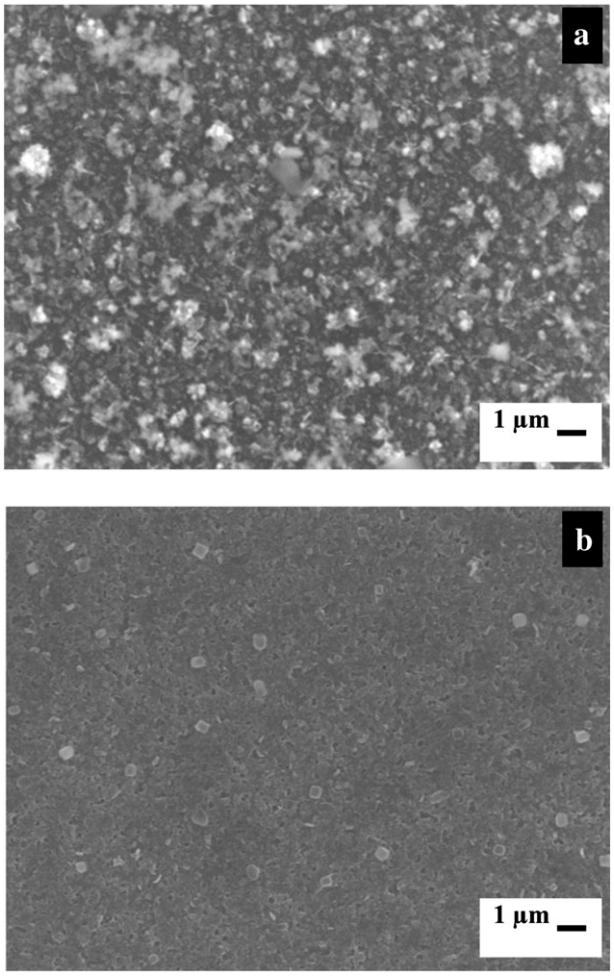

Fig. 3. Top-view FEG-SEM images of the (a) SILAR grown and (b) sol-gel grown CZTS films.

where B is an energy-independent constant, E_g is the optical band-gap energy and m is an index that characterizes the optical absorption process and is theoretically equal to 2 and 1/2 for the indirect and direct allowed transitions, respectively. Fig. 4 shows the absorption behavior (as an inset) and the band-gap photon-energy estimations of the CZTS films, respectively. From the insets of Fig. 4, it can be seen that both films have high absorption coefficient. But compared to the SILAR grown CZTS film, the optical absorption of the sol-gel grown film covered a wider wavelength range by means of absorbing more visible photons. The band-gap estimations were performed by extrapolating the linear region of the plot of $(\alpha h\nu)^2$ versus $h\nu$ to the horizontal axis and considering the intersecting point. As can be seen from Fig. 4, the samples exhibit a linear dependence which indicates the direct band gap nature of the films. Thus we can choose m as 1/2. By plotting the graph of $(\alpha h\nu)^2$ against the photon energy $h\nu$, the band gap values were estimated to be 1.45 and 1.40 eV for the SILAR and sol-gel grown

Table 2
The results of the semi-quantitative, energy-dispersive X-ray spectroscopy (EDXS) analysis.

Element	SILAR grown CZTS		Sol-gel grown CZTS	
	a.f. (%)	$N = 8$[a]	a.f. (%)	$N = 8$[a]
Cu	24.9	2.0	20.1	1.6
Zn	15.6	1.2	16.2	1.3
Sn	12.5	1.0	14.6	1.2
S	47.0	3.8	49.2	3.9
Cu/(Zn + Sn)	0.88		0.65	
Zn/Sn	1.25		1.11	

[a] Composition normalized on 8 atoms per formula unit of CZTS.

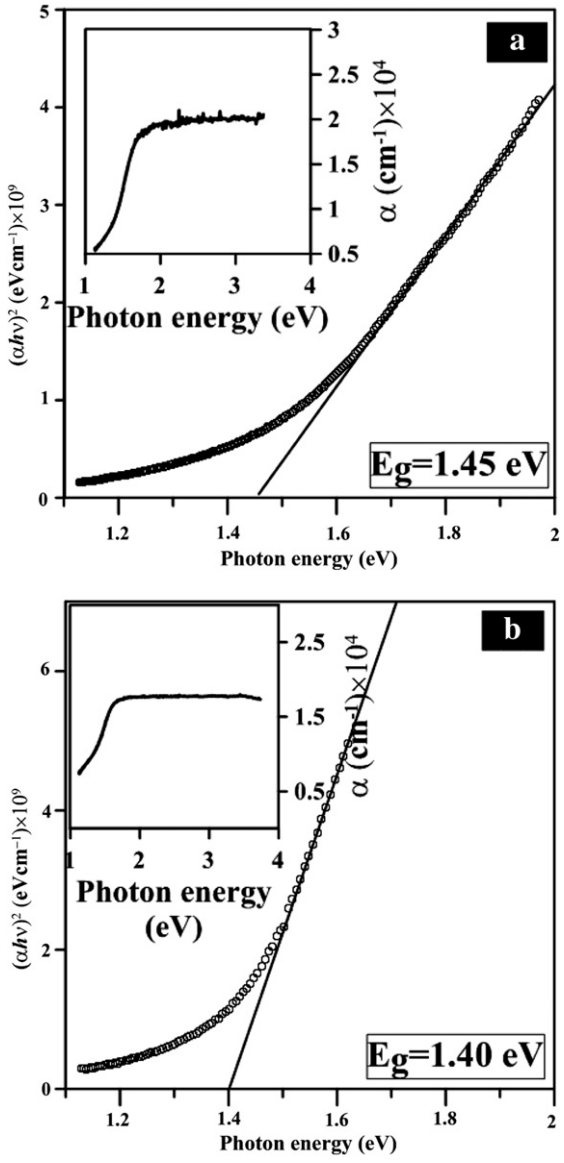

Fig. 4. The band-gap photon-energy estimations and the absorption behavior (as an inset) of the (a) SILAR grown and (b) sol-gel grown CZTS films.

CZTS films, respectively. The E_g value of the CZTS compound, as a p-type direct-band-gap semiconductor, has been reported to be between 1.4 and 1.5 eV [2,6,31,32]. It can be said that the estimated results are quite close to the optimum band gap for a solar cell. The difference between the estimated band gap values may be related to crystallite size, lattice strains, elemental compositions and/or dislocation densities of the studied films.

4. Conclusion

In the present paper, we have investigated CZTS thin films prepared on soda lime glass substrates by SILAR and sol-gel spin coating method. The XRD studies indicated the polycrystalline nature of the films and proved that the crystallization process of the films was carried out. No secondary phases were observed. Mean crystallite size of the SILAR and sol-gel grown films were calculated to be 20 and 9 nm, respectively. It was found that the sol-gel grown CZTS film has smaller crystallite size and relatedly higher micro-strain and dislocation density values than those of SILAR grown CZTS film. Phase purity and good crystalline quality of the studied films were proved through the Raman spectroscopy analyses. From the scanning electron microscopy images, sol-gel grown CZTS film was found to have more homogenous and smooth morphology. Possible chemical formula of the studied films was determined through the elemental composition studies. The values of the optical absorption coefficients of the CZTS films were found to be about 10^4 cm^{-1} via absorbance spectroscopy. Compared to the SILAR grown CZTS film, the optical absorption of the sol-gel grown film covered a wider wavelength range by means of absorbing more visible photons. The optical band gap values were estimated to be 1.45 and 1.40 eV for the SILAR and sol-gel grown samples, respectively, in agreement with previously reported values. It was concluded that both methods are effective and can be used to produce high-quality CZTS thin films for cheap and green solar cell applications.

Acknowledgment

We would like to thank Assist. Prof. Slavko Bernik for helpful discussions and assistance during the study and to Ms. Mateja Podlogar for her support during the characterizations. The financial support from Scientific Research Commission of Mustafa Kemal University (Project No: 1204D0102) is greatly appreciated.

References

[1] K. Ito, T. Nakazawa, Jpn. J. Appl. Phys. 27 (1988) 2094.
[2] H. Katagiri, K. Jimbo, S. Yamada, T. Kamimura, W.S. Maw, T. Fukano, T. Ito, T. Motohiro, Appl. Phys. Express 1 (2008) 041201.
[3] A. Ennaoui, M. Lux-Steiner, A. Weber, D. Abou-Ras, I. Kotschau, H.-W. Schock, R. Schurr, A. Holzing, S. Jost, R. Hock, T. Vob, J. Schulze, A. Kirbs, Thin Solid Films 517 (2009) 2511.
[4] H. Katagiri, K. Saitoh, T. Washio, H. Shinohara, T. Kurumadani, S. Miyajima, Sol. Energy Mater. Sol. Cells 65 (2001) 141.
[5] W. Daranfed, M.S. Aida, N. Attaf, J. Bougdira, H. Rinnert, J. Alloys Compd. 542 (2012) 22.
[6] P.K. Sarswat, M. Snure, M.L. Free, A. Tiwari, Thin Solid Films 520 (2012) 1694.
[7] I. Oja, A. Belaidi, L. Dloczik, M.-Ch. Lux-Steiner, T. Dittrich, Semicond. Sci. Technol. 21 (2006) 520.
[8] A. Fischereder, T. Rath, W. Haas, H. Amenitsch, J. Albering, D. Meischler, S. Larissegger, M. Edler, R. Saf, F. Hofer, G. Trimmel, Chem. Mater. 22 (2010) 3399.
[9] H. Park, Y.H. Hwang, B.S. Bae, J. Sol-Gel Sci. Technol. 65 (1) (2013) 23.
[10] K. Tanaka, N. Moritake, H. Uchiki, Sol. Energy Mater. Sol. Cells 91 (2007) 1199.
[11] M.Y. Yeh, C.C. Lee, D.S. Wuu, J. Sol-Gel Sci. Technol. 52 (2009) 65.
[12] S.S. Mali, B.M. Patil, C.A. Betty, P.N. Bhosale, Y.W. Oh, S.R. Jadkar, R.S. Devan, Y.R. Ma, P.S. Patil, Electrochim. Acta 66 (2012) 216.
[13] Z. Su, C. Yan, K. Sun, Z. Han, F. Liu, J. Liu, Y. Lai, J. Li, Y. Liu, Appl. Surf. Sci. 258 (2012) 7678.
[14] S.S. Mali, P.S. Shinde, C.A. Betty, P.N. Bhosale, Y.W. Oh, P.S. Patil, J. Phys. Chem. Solids 73 (2012) 735.
[15] N.M. Shinde, D.P. Duval, D.S. Dhawale, C.D. Lokhande, J.H. Kim, J.H. Moon, Mater. Res. Bull. 47 (2012) 302.
[16] H. Katagiri, N. Sasaguchi, S. Hando, S. Hoshino, J. Ohashi, T. Yokota, Sol. Energy Mater. Sol. Cells 49 (1997) 407.
[17] S. Chen, X.G. Gong, A. Walsh, S. Wei, Appl. Phys. Lett. 96 (2010) 021902.
[18] P. Fernandes, P. Salome, A. Cunha, J. Phys. D. Appl. Phys. 43 (2010) 215403.
[19] G. Knuyt, C. Quaeyhaegens, J.D. Haen, L.M. Stals, Phys. Status Solidi B 195 (1996) 179.
[20] H.P. Klug, L. Alexander, John Wiley & Sons, New York, 1974.
[21] R. Sathyamoorthy, C. Sharmila, K. Natarajan, S. Velumani, Mater. Charact. 58 (2007) 745.
[22] G.B. Williamson, R.C. Smallman, Philos. Mag. 1 (1956) 34.
[23] J. He, L. Sun, K. Zhang, W. Wang, J. Jiang, Y. Chen, P. Yang, J. Chu, Appl. Surf. Sci. 264 (2013) 133.
[24] C. Gao, H. Shen, F. Jiang, H. Guan, Appl. Surf. Sci. 261 (2013) 189.
[25] O. Zaberca, F. Oftinger, J.Y. Chane-Ching, L. Datas, A. Lafond, P. Puech, A. Balocchi, D. Lagarde, X. Marie, Nanotechnology 23 (2012) 185402.
[26] P.A. Fernandes, P.M.P. Salomé, A.F. da Cunha, Thin Solid Films 517 (2009) 2519.
[27] P.A. Fernandes, P.M.P. Salomé, A.F. da Cunha, J. Alloys Compd. 509 (2011) 7600.
[28] J. Owens, L. Gladczuk, R. Szymczak, P. Dluzewski, A. Wisniewski, H. Szymczak, A. Golnik, C. Bernhard, C. Niedermayer, J. Phys. Chem. Solids 72 (2011) 648.
[29] K. Vipul, K.K. Patel, S.J. Patel, D.V. Shah, J. Cryst. Growth 362 (2013) 174.
[30] J. Tauc, Mater. Res. Bull. 5 (1970) 721.
[31] B.A. Schubert, B. Marsen, S. Cinque, T. Unold, R. Klenk, S. Schorr, H.W. Schock, Prog. Photovolt. Res. Appl. 19 (2011) 93.
[32] J.S. Seol, S.Y. Lee, J.C. Lee, H.D. Nam, K.H. Kim, Sol. Energy Mater. Sol. Cells 75 (2003) 155.